Onset of Faraday Waves in a Liquid Layer Covered with a Surfactant with Elastic and Viscous Properties

María D. Giavedoni*,[†] and Sebastián Ubal[†,‡]

INTEC, CONICET−Universidad Nacional del Litoral, Güemes 3450, 3000 Santa Fe, Argentina, and Facultad de Ingeniería, Universidad Nacional de Entre Ríos, Ruta Prov. 11, km 10, 3101 Oro Verde, Entre Ríos, Argentina

In this work, we analyze the formation of Faraday waves on the free surface of a liquid layer covered by an insoluble surfactant. The linear analysis that is conducted includes the effects of both surface elasticity and surface viscosity. The critical force needed to form the waves, as well as the critical wavenumber, are determined within a large range of values of the dimensionless parameters representing the physicochemical properties of the surfactant. The examination of carefully selected hydrodynamic variables provides further insight into the behavior of the system.

1. Introduction

This paper is concerned with the conditions for the onset of Faraday waves at the interface of a liquid layer covered with a surface active agent that confers viscous and elastic properties to the free surface. The phenomenon of Faraday waves refers to the standing waves formed on the free surface of a horizontal liquid layer undergoing a oscillatory vertical acceleration, produced by the vibration of the container.[1] When the driving acceleration ranges from weak to moderate, several types of wave patterns, such as rolls, squares, or hexagons, are exhibited.[2−4] However, if the vibration of the container is strong enough, the rupture of the free surface and the ejection of liquid drops into the gas phase can be observed.[5,6]

The analysis of this physical phenomenon has practical interest in spray formation where a controlled/predictable drop size and flow rate are usually desired. Particular applications include mass-transfer processes, air humidification, ultrasonic nebulizers, and fuel injection systems. The study of this problem is also of interest in fundamental topics with wide applications in chemical engineering such as nonlinear dynamics and pattern formation.

The presence of surface-active agents is ubiquitous at most gas/liquid interfaces, either as additives or as uncontrolled contaminants. Whatever the case, these adsorbed substances have a pronounced effect on the interfacial balance of stresses, and this, in turn, affects the bulk flow. In fact, when a surfactant is adsorbed at the interface, the forces acting on the free surface include surface tension gradients and viscous resistance to shear and dilatation.

The objective of this work is to investigate the influence of the physicochemical properties of an insoluble surfactant adsorbed at the liquid surface on the critical conditions for the formation of Faraday waves. The elastic effects of a surface-active agent on Faraday waves were examined in the literature experimentally, analytically, and numerically. Henderson[7] measured the damping rates, natural frequencies, and amplitudes of the fundamental axisymmetric wave formed in a cylindrical container partially filled with water covered with an insoluble

film of a surfactant; she also compared the experimental values with existing theoretical models. Decent[8] analyzed the nonlinear damping of Faraday waves using an evolution equation; in his study, he considered the surface boundary layer produced by an inextensible surface film. Kumar and Matar[9,10] presented a full linear stability analysis of the problem valid for liquids of arbitrary depth and viscosity, when the effect of the lateral boundaries is negligible. Matar et al.[11] examined the evolution of a thin liquid layer, clean or covered by a surfactant film, in the nonlinear regime. To this end, they numerically solved the set of nonlinear differential equations previously derived by them[12] using lubrication theory. Ubal et al.[13] presented a numerical analysis of the full nonlinear problem in which the conditions for the onset of the instability and the evolution of the interfacial variables, as a function of the elastic number, are determined and discussed. The results of the studies previously mentioned indicate that the critical forcing acceleration needed to induce standing waves in a contaminated surface is larger than that in a clean surface, although the critical vibration force shows a nonmonotonical dependence on the elasticity of the adsorbed film. In addition, all the studies reveal the existence of a temporal phase shift between the evolution of the surface elevation and surfactant concentration, which changes with the elastic number in a similar way to the applied force.

Surface viscous effects have received considerably less attention in the literature; Ubal et al.[14] numerically investigated the role of surface viscosity on the onset of the Faraday instability, assuming that the interfacial properties are independent of the surfactant concentration, i.e., neglecting the effect of the surface elasticity. These authors found that the minimum force required to form the waves increases with surface viscosity in a sigmoidal fashion; that is, the threshold acceleration is almost constant at very low and very high values of that interfacial property.

In the present work, the combined influence of surface elasticity and viscosity on the onset conditions for the development of standing waves is examined. To this end, the linear stability analysis presented by Kumar and Matar[9] is extended to account for interfacial viscosity. We also show that the evaluation of carefully selected interfacial properties is useful for a better understanding of the phenomena. The paper is organized as follows. In the next section, the mathematical

---

* To whom correspondence should be addressed. Tel.: +54 342 4559174. Fax: +54 342 4550944. E-mail address: madelia@ceride.gov.ar, madelia@ceride.gov.ar, subal@ceride.gov.ar.
† INTEC, CONICET−Universidad Nacional del Litoral.
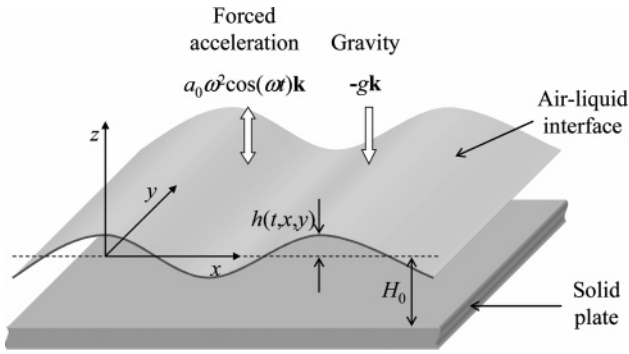‡ Facultad de Ingeniería, Universidad Nacional de Entre Ríos.

Figure 1. Sketch of the domain and coordinate system adopted.

formulation of the problem is presented. In section 3, the results for a wide range of values of the parameters are shown. Finally, some concluding remarks are given in section 4.

2. Mathematical Formulation

2.1. Governing Equations. Let us consider a liquid layer of depth H_0 lying on a horizontal solid surface. The density (ρ) and viscosity (μ) of the fluid are constant, and the air above it is regarded as inviscid. A monolayer of an insoluble surfactant is adsorbed at the gas/liquid interface and is responsible for the viscous and elastic properties exhibited by the free surface. The system is subjected to a vertical periodic motion; depending on its angular frequency (ω) and amplitude (a_0), this vibration can set the liquid in motion and lead to the formation of surface waves. Therefore, the dynamics of the fluid in the bulk is governed by the Navier–Stokes and continuity equations, which, in a coordinate system moving with the unperturbed interface (see Figure 1), are written as follows:

$$\rho\left(\frac{\partial \mathbf{v}}{\partial t} + \mathbf{v}\cdot\nabla\mathbf{v}\right) = -\nabla p + \mu\nabla^2\mathbf{v} + \rho(\mathbf{g} + \mathbf{a}) \tag{1}$$

$$\nabla\cdot\mathbf{v} = 0 \tag{2}$$

where $\mathbf{a}$ is the specific body force which, in the noninertial frame of reference selected, is equivalent to a modulated gravitational acceleration ($\mathbf{a} = a_0\omega^2 \cos(\omega t)\mathbf{k}$).

On the bottom surface, the no-slip boundary condition applies:

$$\mathbf{v} = 0, \quad z = -H_0 \tag{3}$$

Because of the fact that the liquid/air interface is a material surface, the usual form of the kinematic condition is imposed:

$$\frac{\partial h}{\partial t} + u\frac{\partial h}{\partial x} + v\frac{\partial h}{\partial y} = w, \quad z = h(t, x, y) \tag{4}$$

where u and v are the x- and y-components of the velocity vector, respectively, and $h(t,x,y)$ is the deviation of the free surface shape from the flat configuration at rest. Stresses at the interface are counterbalanced by surface traction; that is,[15,16]

$$\mathbf{n}\cdot\mathbf{T} = \nabla\cdot\mathbf{T}^S, \quad z = h(t, x, y) \tag{5}$$

where $\mathbf{n}$ is the external unit normal to the interface, and $\mathbf{T}$ and $\mathbf{T}^S$ are the bulk and surface stress tensors, respectively. Surfactants adsorbed at the interface are responsible for the viscous and elastic properties exhibited by the free surface. We assume that the interface is a Newtonian surface; hence, the surface stress tensor is given by the Boussinesq–Scriven equation:[17]

$$\mathbf{T}^S = [\sigma + (\kappa^S - \mu^S)\nabla_S\cdot\mathbf{v}^0]\mathbf{I}^S +$$
$$\mu^S[\nabla_S\mathbf{v}^0\cdot\mathbf{I}^S + \mathbf{I}^S\cdot(\nabla_S\mathbf{v}^0)^T] \tag{6}$$

In eq 6, σ is the surface tension; κ^S and μ^S are the dilatational and shear viscosity coefficients, respectively; $\mathbf{I}^S = \mathbf{I} - \mathbf{nn}$ is the surface identity tensor; $\mathbf{v}^0$ is the interfacial velocity ($\mathbf{v}^0 = v^{0s}\mathbf{t} + v^{0n}\mathbf{n}$, with $\mathbf{t}$ being a unit vector tangential to the free surface); and $\nabla_S = \mathbf{I}^S\cdot\nabla$ is the surface gradient operator.

The surface tension and the surface viscosity coefficients are dependent on the concentration of the solute adsorbed at the interface (ρ^S); because of the fact that this work involves the linear stability of the system, linear equations of state suffice to describe the variations of these interfacial properties with the surfactant concentration. Thus, we have

$$\sigma = \sigma_0 + \left(\frac{\partial\sigma}{\partial\rho^S}\right)_0 (\rho^S - \rho_0^S) \tag{7}$$

$$\mu^S = \mu_0^S + \left(\frac{\partial\mu^S}{\partial\rho^S}\right)_0 (\rho^S - \rho_0^S) \tag{8}$$

$$\kappa^S = \kappa_0^S + \left(\frac{\partial\kappa^S}{\partial\rho^S}\right)_0 (\rho^S - \rho_0^S) \tag{9}$$

where ρ_0^S is the concentration of surfactant at equilibrium (i.e., at the flat interface); σ_0, μ_0^S, and κ_0^S are the surface tension and the coefficients of shear and dilatational viscosity evaluated at ρ_0^S. The subscript in the operator $(\partial/\partial\rho^S)_0$ indicates that the derivative is computed at equilibrium. To complete the formulation of the problem, a mass balance for the surfactant adsorbed at the interface is needed; for an insoluble solute, that balance is[18]

$$\left.\frac{\partial\rho^S}{\partial t}\right|_n + \nabla_S\cdot(\rho^S\mathbf{v}^0) - D^S\nabla_S^2\rho^S = 0 \tag{10}$$

where D^S is the surfactant surface diffusion coefficient, ∇_S^2 the surface Laplacian operator ($\nabla_S^2 = \nabla_S\cdot\nabla_S$), and $\partial/\partial t|_n$ a time derivative following the motion of the free surface along its normal direction.

2.2. Scaling and Linearization. Before performing the linearization process, a proper dimensionless formulation of the problem is convenient. To this end, the characteristic scales chosen are $1/\omega$ for time, $l_C = g/\omega^2 + (\sigma/\rho\omega^2)^{1/3}$ for length, $l_C\omega$ for velocity, ρ_0^S for surfactant concentration, and $\rho a_0\omega^2 l_C$ for pressure. To select l_C, we considered the well-known fact that the wavelength of Faraday waves diminishes as the external frequency is augmented: at low frequencies, typical wavelengths are of the order of g/ω^2, whereas at high frequencies, they are of the order of $[\sigma/(\rho\omega^2)]^{1/3}$. Therefore, the aforementioned choice for l_C is suitable at high (capillary waves), low (gravity waves), and intermediate frequencies.

The dimensionless governing equations then are linearized for small perturbations of the equilibrium state; that is, $\mathbf{v} = 0$, $p = -\rho z[g - a_0\omega^2 \cos(\omega t)]$, $h(t,x,y) = 0$, and $\rho^S = \rho_0^S$. After some algebraic manipulation (similar to that employed in ref 9), the following set of equations results:

$$\frac{\partial\mathbf{v}}{\partial t} = -A\nabla p + \frac{1}{Re}\nabla^2\mathbf{v} \tag{11}$$

$$\nabla\cdot\mathbf{v} = 0 \tag{12}$$

$$\mathbf{v} = 0, \quad z = z_p \tag{13}$$

$$\frac{\partial w}{\partial z} = 0, \quad z = z_p \tag{14}$$

$$\frac{\partial h}{\partial t} = w, \quad z = 0 \tag{15}$$

$$B[1 - F\cos t]h - BFp + 2Ca\frac{\partial w}{\partial z} = \nabla_H^2 h, \quad z = 0 \tag{16}$$

$$\left(\frac{\partial u}{\partial z} + \frac{\partial w}{\partial y}\right)\mathbf{i} + \left(\frac{\partial v}{\partial z} + \frac{\partial w}{\partial y}\right)\mathbf{j} = -M_a\nabla_H\gamma +$$
$$Bo_\kappa\nabla_H(\nabla_H\cdot\mathbf{v}_H^0) + Bo_\mu\nabla_H^2\mathbf{v}_H^0, \quad z = 0 \tag{17}$$

$$\left(\frac{\partial\gamma}{\partial t}\right)_n + \nabla_H\cdot\mathbf{v}_H^0 - \frac{1}{Pe_S}\nabla_H^2\gamma = 0, \quad z = 0 \tag{18}$$

In the aforementioned expressions, dimensionless variables are represented by the same symbols as the corresponding dimensional ones, with the exception of the dimensionless concentration of surfactant, which is defined as $\gamma = \rho^S/\rho_0^S$. Also, w is the z-component of the velocity, and ∇_H and ∇_H^2 are the gradient and Laplacian operators in the x-y plane, respectively ($\nabla_H = (\mathbf{ii} + \mathbf{jj})\cdot\nabla$ and $\nabla_H^2 = \nabla_H\cdot\nabla_H$). The dimensionless parameters appearing in eqs 11−18 are the Reynolds number ($Re = \rho\omega l_C^2/\mu$), the capillary number ($Ca = \mu\omega l_C/\sigma_0$), the Bond number ($B = l_C^2\rho g/\sigma_0$), the shear and dilatational Boussinesq numbers ($Bo_\mu = \mu_0^S/l_C\mu$ and $Bo_\kappa = \kappa_0^S/l_C\mu$), the Marangoni number ($Ma = \beta/Ca$, where $\beta = -(\rho_0^S/\sigma_0)(\partial\sigma/\partial\rho^S)_0$ is the elastic number), the Péclet number ($Pe_S = \omega l_C^2/D^S$), the ratio between the forced and gravity accelerations ($F = a_0\omega^2/g$), the dimensionless depth of the liquid layer ($z_P = -H_0/l_C$), and the dimensionless amplitude of the vibration ($A = a_0/l_C = BF/ReCa$). Equations 16 and 17 are the linear forms of the normal and tangential components of the surface traction, respectively. A careful inspection of these two expressions reveals that they are independent of local variations of the surfactant concentration, when the elasticity number is negligible.

2.3. Solution of the Linear Problem. The original set of variables of the problem can be reduced to a smaller one (w, h, and γ), by eliminating p, u, and v by means of the usual algebraic procedure.[19] Because we are considering the formation of standing waves on the surface of a liquid layer that extends infinitely in the x−y plane, the solution can be expressed in terms of normal modes of the form $\exp(i\,\mathbf{k}\cdot\mathbf{x})$, where $\mathbf{k} = k_x\mathbf{i} + k_y\mathbf{j}$ is the wave vector. Moreover, because the system is forced with a 2π-period excitation and a periodic solution is expected, Floquet theory can be applied; therefore, the time evolution of the variables can be expressed as a linear combination of time-periodic modes of the form $\exp[(s + i\delta)t]\exp(int)$, with $(s + i\delta)$ being the Floquet exponent: s is the growth rate, and δ is equal to 0 or $^1/_2$ for the harmonic and subharmonic solutions, respectively. We then can write

$$w(t, x, y, z) = e^{i\mathbf{k}\cdot\mathbf{x}}\sum_{n=-\infty}^{n=\infty}\hat{w}_n(z)\exp\{[s + i(\delta + n)]t\} \tag{19}$$

$$h(t, x, y) = e^{i\mathbf{k}\cdot\mathbf{x}}\sum_{n=-\infty}^{n=\infty}\hat{h}_n\exp\{[s + i(\delta + n)]t\} \tag{20}$$

$$\gamma(t, x, y) = e^{i\mathbf{k}\cdot\mathbf{x}}\sum_{n=-\infty}^{n=\infty}\hat{\gamma}_n\exp\{[s + i(\delta + n)]t\} \tag{21}$$

With an algebraic procedure similar to that applied by Kumar and Matar,[9] the following recursion relationship can be obtained:

$$A_n\hat{h}_n + B_n\hat{\gamma}_n = \frac{BF}{2Ca}k^2(\hat{h}_{n-1} + \hat{h}_{n+1}) \tag{22}$$

where

$$A_n = \frac{B + k^2}{Ca} + \frac{q_n^2 - k^2}{\text{DENO}}\left[-4kq_n(k^2 + q_n^2) + \right.$$
$$\frac{q_n}{k}(5k^4 + q_n^4 + 2k^2q_n^2)\cosh(kz_P)\cosh(q_nz_P)-$$
$$(k^4 + q_n^4 + 6k^2q_n^2)\sinh(kz_P)\sinh(q_nz_P) +$$
$$Bokq_n(q_n^2 - k^2)(q_n\cosh(kz_P)\sinh(q_nz_P) -$$
$$\left. k\sinh(kz_P)\cosh(q_nz_P))\right] \tag{23}$$

$$B_n = \frac{MaRek}{\text{DENO}}\{-q_n(3k^2 + q_n^2)[1 - \cosh(kz_P)\cosh(q_nz_P)] -$$
$$k(k^2 + 3q_n^2)\sinh(kz_P)\sinh(q_nz_P)\} \tag{24}$$

The definition of the dummy variable DENO is given in the Appendix, (see eq A-5). Also, k is the horizontal dimensionless wavenumber ($k = (k_x^2 + k_y^2)^{1/2}$), $q_n^2 = k^2 + iRe(\delta + n)$, and $Bo = Bo_\kappa + Bo_\mu$. Bo is the only parameter that accounts for the surface viscosity of a standing wave of the form $\exp(i\,\mathbf{k}\cdot\mathbf{x})$. The relationship between $\hat{h}_n$ and $\hat{\gamma}_n$ is obtained from the surfactant mass balance (eq 18) and is given by

$$\hat{\gamma}_n = G_n\hat{h}_n \tag{25}$$

where

$$G_n = (k(q_n^2 - k^2)\{-q_n(3k^2 + q_n^2)$$
$$[1 - \cosh(kz_P)\cosh(q_nz_P)] -$$
$$k(3q_n^2 + k^2)\sinh(kz_P)\sinh(q_nz_P)\}) \div$$
$$[Re([(Bok^3/Pe_S) + (Bok(q_n^2 - k^2)/Re) +$$
$$Mak]e_n + (q_n^2 - k^2)\{(k^2/Pe_S) + [(q_n^2 - k^2)/Re]\}f_n)] \tag{26}$$

The coefficients e_n and f_n are defined in the Appendix (see eqs A-7 and A-6). The reader can easily verify that the aforementioned expressions reduce to those obtained by Kumar and Matar[9] when the surface viscosity is zero (i.e., $Bo = 0$).

The recursive expression (eq 22) can be written as a complex semi-infinite matrix system for both the harmonic ($\delta = 0$) and subharmonic ($\delta = ^1/_2$) cases. Specifying the values of the dimensionless parameters Re, Ca, B, Ma, Pe_S, Bo, and z_P, choosing a wavenumber k, setting the growth rate s equal to 0, and truncating the matrix system at a finite value of n, an eigenvalue problem for the critical driving force F results. The numerical tests performed show that $n = 10$ is large enough to ascertain the invariance of the results. Next, we discuss the solutions computed with the technique just described.

3. Results and Discussion

In this section, the onset conditions for the formation of Faraday waves on the free surface of a 0.0015-m-deep liquid layer subjected to a 120 Hz vertical oscillation are determined. The density and viscosity of the liquid are those of pure water at 20 °C, and the surface tension of the interface at equilibrium is equal to 0.070 N/m. Thus, $Re = 199.8$, $Ca = 0.005$, $B =$
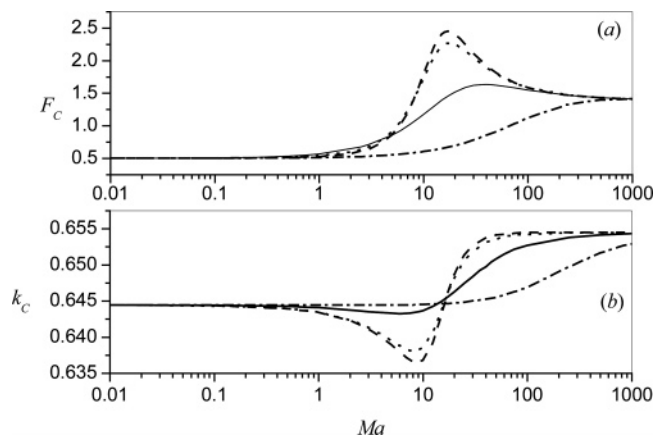
Figure 2. (a) Critical dimensionless acceleration and (b) critical wave-number, each as a function of the Marangoni number (Ma) for negligible surface viscosity and surface Peclet number (Pe_S) values of $(-\cdot-)$ 0.0799, $(-)$ 0.799 , $(\cdot\cdot)$ 7.99, and $(---)$ 7.99 $\times$ 10^4. Other parameters of the system are $Re = 199.8$, $Ca = 0.0055$, $B = 0.0371$, and $z_P = -2.914$.

0.0371, and $z_P = -2.914$. The properties of the surfactant (i.e., surface diffusivity and the elastic and viscous coefficients) vary widely.

To establish the critical values of the dimensionless acceleration (F_C) and the wave number (k_C), the stability maps on the $F-k$ plane were constructed for each selected set of the characteristic numbers of the system. From these maps, we concluded that the first instability is always the subharmonic response; therefore, the results presented here are only for that mode.

To better understand the action of a surfactant on the dynamics of the system, we discuss the separate effects of surface elasticity and surface viscosity before analyzing their combined activity on the formation of the waves.

3.1. Surface Elasticity. The main objective of the following analysis is twofold: (i) to compare the solutions obtained with the recurrence relation described by eq 22 in the limit of zero surface viscosity with those previously reported by Kumar and Matar;[9,10] and (ii) more important, to get a deeper insight of the problem through the analysis of selected interfacial variables. With this purpose, the elastic number was varied between 0 and 5.5, which, in the present analysis, is equivalent to modifying the Marangoni number within the range of $Ma = 0-1000$. Because of the fact that the elastic modulus typically is between 0 (clean interface) and ~0.1 N/m, the parameter Ma could vary from 0 to ~260 for real surfactants and the physical parameters stated at the beginning of section 3. On the other hand, some of the few published values of the surface diffusion coefficient are on the order of 10^{-10} m^2/s; thus, the resulting Pe_S value is ~2 $\times$ 10^6.

In Figure 2a and b, we depict the trends followed by F_C and k_C with Ma for four different Pe_S values; it is easily verified that these results are in very good agreement with those given in refs 9 and 10. All the curves are independent of Pe_S, either for very large or very small Ma; besides, F_C has a maximum that becomes less significant and moves toward larger Ma as the ratio between surface diffusion and surface convection increases. Moreover, this maximum is not longer observed when $Pe_S \ll 1$. Whenever the maximum is present, the critical wavenumber shows a minimum that becomes less pronounced and moves toward lower values of Ma as Pe_S diminishes.

The studies about the effects that an insoluble surfactant has on the damping coefficient of free surface waves establish that this quantity increases nonmonotonically with surface elasticity.
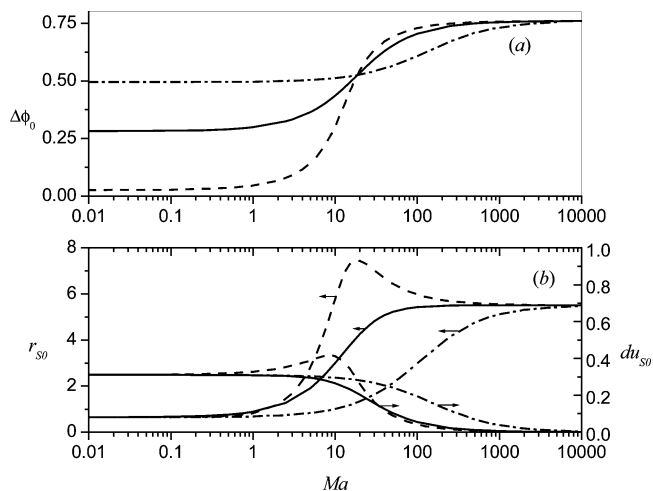
Figure 3. (a) Phase difference between $\hat{\gamma}_0$ and $\hat{h}_0$, $\Delta\phi_0$, as a function of Ma; (b) amplitude of the tangential surface stretching, du_{S_0}, and magnitude of the curl of the surface velocity, r_{S_0}, vs Ma; $Pe_S = (-\cdot-)$ 0.0799, $(-)$ 0.799, and $(---)$ 7.99 $\times$ 10^4 $(-)$. Other parameters of the system are the same as those described in Figure 2.

Levich[20] performed an approximate linear analysis of this problem and derived an expression for the damping coefficient as a function of the parameters of the system; nevertheless, he only studied the two limit situations in which elastic effects are either negligible or very large. From the expression obtained by this author, it is easily verified that the damping coefficient presents a maximum at $\beta_C \approx 2\mu\alpha^2/(\rho\omega_0)$, where α is the wavenumber and ω_0 is the natural frequency of the wave. This result is valid for capillary waves, slightly viscous fluids, and when surface diffusion is negligible.

The minimum force required to form the waves will be larger if the damping coefficient increases; thus, the largest value of F_C should be connected to the highest value of this variable. If the above expression for β_C is evaluated for the particular case considered in this work, with $\alpha \approx 1266.3$ m^{-1} (a value resulting from the dispersion relationship for inviscid capillary waves), we obtain $\beta \approx 0.09$. The computed solutions of the linear problem illustrated in Figure 2 show that F_C is maximum when $\beta = 0.094$ ($k_C = 1254.5$ m^{-1}) and 0.092 ($k_C = 1262.2$ m^{-1}), for $Pe_S = 7.991 \times 10^4$ and 0.7991, respectively.

A more-detailed analysis of the behavior of the system requires a closer inspection of the interfacial variables. In this work, we followed the phase difference between the temporal evolution of the interfacial concentration of surfactant and the free surface deflections measured in units of π,

$$\Delta\phi_0 = \text{angle}(\hat{\gamma}_0) - \text{angle}(\hat{h}_0)$$

the amplitude of the tangential surface stretching,

$$du_{S0} = |\nabla_H \cdot \mathbf{v}^0|$$

and the magnitude of the curl of the surface velocity,

$$r_{S0} = |\nabla_H \times \mathbf{v}^0|$$

For the sake of simplicity, all these variables were calculated for two-dimensional waves (rolls), and details of the calculations are given in the Appendix. Results illustrated in Figure 3a and b show that those variables are almost constant for very small and very large Ma values, in agreement with the trend followed by F_C.
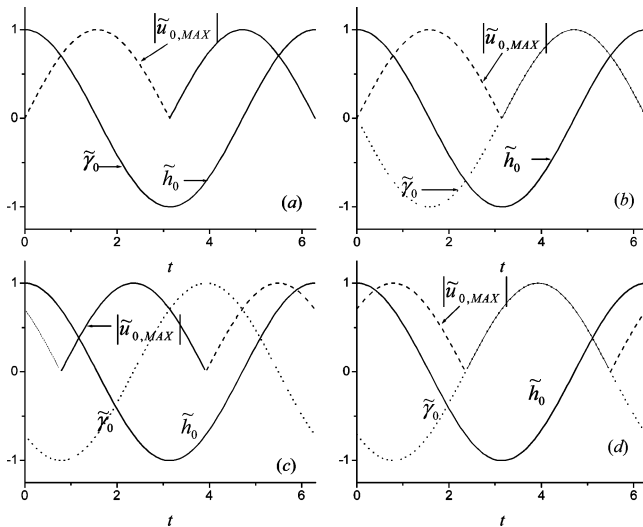
Figure 4. Schematic representation of the temporal evolution during a cycle of $\tilde{h}_0$ and $\tilde{\gamma}_0$, and $|\tilde{u}_{0,MAX}|$. Panels a and b correspond to an inert solute when mass transport is controlled by convection or diffusion, respectively; panels c and d correspond to a surfactant in the limit of very large and very small Pe_S, respectively.

To provide a better understanding of the phase shift between the evolution of the local concentration of surfactant and the free surface deflections, we will first discuss the case corresponding to an inert solute. In this particular situation, the fluid mechanic problem is not dependent on local variations of the solute concentration; however, to evaluate the distribution of solute along the free surface, the interfacial velocity must be introduced in eq 18. Two limiting situations regarding the mass balance of solute can be considered: (i) transport controlled by convection and (ii) transport controlled by diffusion. These two cases are examined next, in connection with $\Delta\phi_0$, with the help of eqs A-14 and A-15 in the Appendix and Figure 4, where the temporal evolutions of the dominant modes of the free surface height,

$$\tilde{h}_0 \equiv \mathrm{Re}\!\left[\hat{h}_0 \exp\!\left(\frac{i}{2t}\right)\right]$$

and the local concentration of solute,

$$\tilde{\gamma}_0 \equiv \mathrm{Re}\!\left[\hat{\gamma}_0 \exp\!\left(\frac{i}{2t}\right)\right]$$

(at a point A of the free surface that, at $t = 0$, is at the crest of a wave whose trough is located at point B), and the maximum absolute value of the dominant mode of the tangential component of the free surface velocity,

$$|\tilde{u}_{0,\mathrm{MAX}}| \equiv \left|\mathrm{Re}\!\left[-i\hat{u}_{\mathrm{H}_0}(0)\exp\!\left(\frac{i}{2t}\right)\right]\right|$$

which occur between points A and B, are sketched.

It is easy to see that, when the deformation of the free surface is maximum, $|\tilde{u}_{0,\mathrm{MAX}}|$ is equal to zero, and that when the free surface is flat, $|\tilde{u}_{0,\mathrm{MAX}}|$ is maximum. In case (i), the local concentration of solute is dependent only on the convective transport (see eq 18); therefore, the motion of the solute will have the same direction as the tangential component of the surface velocity, and the evolution of the free surface height and the local concentration of solute will be in phase, which is a result that can be easily derived from eqs A-14 and A-15 from the Appendix when $Pe_S \gg 1$. Therefore, at the initial time

considered in Figure 4, the free surface will be rich in solute at A and it will be depleted at B, whereas, at $t = \pi$, the opposite situation will occur. During the time elapsed between these two instants of the cycle, convection transports solute from A to B, reversing the concentration gradient. When the strength of convection is maximum (the interface is flat), the distribution of solute becomes uniform.

In case (ii), diffusion opposes to convection. Therefore, as the concentration gradient is formed, solute will diffuse in the direction opposite from that in which it is convected. This will produce a phase shift between the evolution of the interfacial distribution of solute and the motion of the liquid in the bulk (or the free surface deflections). The question is what is the maximum value of the phase shift that can be associated with diffusion. The origin of a nonuniform distribution of solute is convection; when diffusion is very large, one expects that this mechanism will be able to restore a uniform concentration when the convective transport is negligible (at $t = 0$ and π in Figure 4a) and that the maximum concentration gradient will occur when convection is maximum (at $t = 0.5\pi$ and 1.5π in Figure 4a). Therefore, the maximum phase angle difference between the evolution of the distribution of solute and the free surface deflections will be as large as 0.5 when $Pe_S \ll 1$ and the solute is not a surfactant (see Figure 4b). This result can also be obtained from eqs A-14 and A-15 in the Appendix.

The previous reasoning is confirmed by results illustrated in Figure 3a. In fact, for a very weak surfactant ($Ma \ll 1$), $\Delta\phi_0 \approx 0$ and 0.5 when $Pe_S = 7.99 \times 10^4$ and 0.0799, respectively; also it is easy to conclude from eqs A-14 and A-15 in the Appendix and the results of Figure 3a that regardless of the Pe_S value, the flow in the bulk is in phase with the flow along the interface when $Ma = Bo = 0$. Curves that are depicted in the figure also show that $\Delta\phi_0$ monotonically increases as Ma is augmented until it becomes ~ 0.75 for the three Pe_S values considered. From the aforementioned discussion about the values of the phase shift for an inert solute, we can conclude that, if $\Delta\phi_0 > 0.5$, the convective transport of surfactant will change direction before the motion of the liquid in the bulk is reversed.

Let us first consider the case corresponding to $Pe_S = 0.07991$. When Ma is small, the largest concentration gradient is formed when the convective transport is largest, i.e., when the free surface is a horizontal plane. Then, at this instant of the cycle, the Marangoni traction produces its maximum effect on the interfacial velocity, slowing the motion of the liquid from the trough to the crest of the wave; therefore, the tangential velocity turns to zero before the free surface attains its maximum deformation. If we assume that the effect of diffusion remains practically the same as β increases—which is a hypothesis supported by the fact that the solutions obtained (not reported here) indicate that $\hat{\gamma}_0$ diminishes as Ma is augmented—we conclude that the increase in $\Delta\phi_0$ from 0.5 to 0.75 results from a phase shift between the motion of the liquid along the interface and that in the bulk phase. This situation is depicted in Figure 4d.

Following similar reasoning, we can conclude that, for $Pe_S = 7.991 \times 10^4$ and sufficiently large β, the phase shift between the evolutions of $\hat{\gamma}_0$ and $\hat{h}_0$ results from a phase shift between the motions of the liquid in the bulk and along the interface that is ~ 0.75 (see Figure 4c).

Numerical solutions of the fully nonlinear problem previously reported[13] qualitatively agree with the aforementioned discussion. In fact, the phase shift between the evolutions of the free surface deflection and the tangential component of the surface velocity increases as β is augmented.
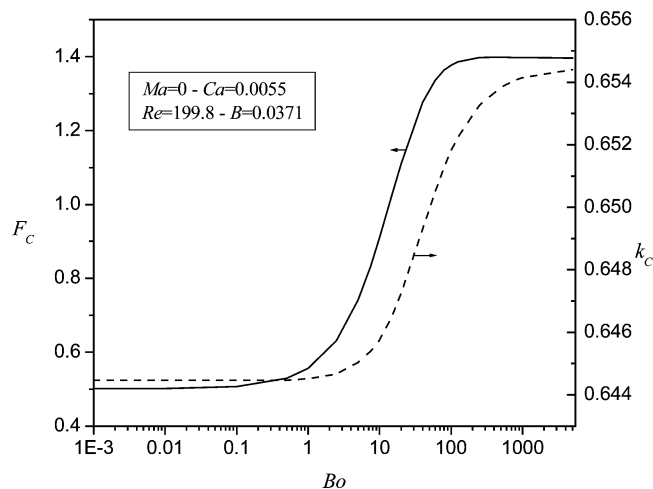
Figure 5. Dimensionless critical force and wavenumber, as a function of the Boussinesq number (Bo) when elastic effects are negligible.

Figure 6. (a) Amplitude of the tangential surface stretching, du_{S_0}, and magnitude of the curl of the surface velocity, r_{S_0}, versus Ma; (b) phase difference between $\hat{\gamma}_0$ and $\hat{h}_0$, $\Delta\phi_0$, as a function of Ma for $Pe_S = 7.99 \times 10^4$.
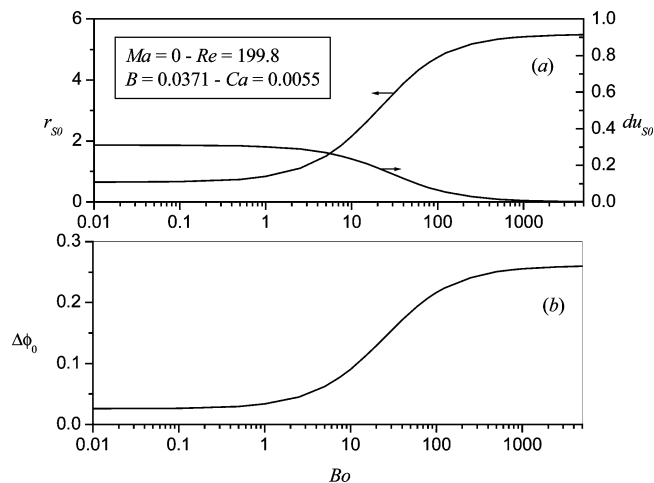
The magnitude of the curl of the surface velocity can be associated with viscous dissipation at the free surface (see, for instance, eqs 21 and 1.15 of ref 20). Thus, the larger the F_C value, the larger the r_{S_0} value. A comparison of the curves depicted in Figures 2a and 3b, for $Pe_S = 7.991 \times 10^4$ and 0.07991, shows that F_C and r_{S_0} are indeed correlated. In all three cases, the value achieved by r_{S_0} at large Ma is ~10 times greater than its value when elastic effects are negligible, whereas the F_C value only increases by a factor of 3.

The ultimate effect of surface elasticity is to make the deformation of the free surface very similar to that of an incompressible solid plate. This fact can easily be concluded, observing that du_{S_0} is almost zero for $Ma \geq 1000$ (see Figure 3b), and that $u = 0$ at the trough and at the crest of the waves. A salient feature of the curves of du_{S0} vs Ma is the maximum presented when $Pe_S = 7.991 \times 10^4$, which occurs at $Ma = 9$, that is, simultaneously with the minimum observed in k_C for the same value of Pe_S (see Figure 2b). It is interesting to note that the inextensible behavior of the free surface when $Ma \gg 1$ has been exploited by Huber et al.[22] to analyze the formation of Faraday waves on the free surface of normal alkane under surface freezing conditions.

3.2. Surface Viscosity. To assess the effect of surface viscosity on the formation of Faraday waves, we computed the solution of the linear problem over a large range of Bo values. The largest value assigned to this parameter ($Bo = 10^4$) represents a system in which the viscosity of the free surface is equal to 5.15×10^{-3} Pa m s, that is, 5.15 times greater than the viscosity of the liquid in the bulk. Typical Bo values could be between 0 (for a surfactant-free interface) and 1.3×10^6 (when calculated using $\mu_S + \kappa_S \approx 0.65$ N s/m).

As we already noted, the system of eqs 11−18 indicates that, when the surface tension is constant, the interfacial viscosity creates a nonzero tangential component of the surface traction that opposes nonhomogeneous deformations of the interface (see eq 17). Besides, in this event, the velocity and pressure fields, as well as the amplitude of the free surface, are independent of the interfacial concentration of surfactant ($B_n = 0$; see eq 24).

The curves of F_C and k_C, as a function of Bo, are very similar (see Figure 5): both variables remain constant for small Bo and then they experience a sharp increase to attain a value that remains constant and is equal to that reported in the previous section for $Ma \rightarrow \infty$ and $Bo = 0$. The effect of increasing surface viscosity is first noticed in F_C and then in k_C; that is, a behavior

opposite to that described in Figure 2 for surface elasticity. Also, neither the absolute maximum presented by F_C nor the absolute minimum exhibited by k_C vs Ma, when $Pe_S > 1$, are observed here.

To further discuss the effects that surface viscosity has on the system, we calculated the phase difference between the interfacial concentration of surfactant and the temporal evolution of the free surface deflections, the amplitude of the tangential surface stretching, and the magnitude of the curl of the surface velocity for $0 \leq Bo \leq 5000$. The results are illustrated in Figure 6a and b for Bo within the range of 0.01−5000, because no significant changes are noticed for smaller Bo.

The effect of increasing viscous effects on these variables is quite similar to the effect of increasing the elastic number. Both du_{S_0} and r_{S_0} are monotonic functions of Bo; they are almost constant at both low and large Bo. The magnitude of du_{S_0} decreases and approaches zero as the surface viscosity increases, noting that the velocity distribution becomes smoother as Bo increases; moreover, at large values of this parameter, the deformation of the free surface is similar to that of a solid plate. The magnitude of r_{S_0} increases with Bo until it becomes approximately equal to 10 times the value corresponding to a clean interface, when $Bo \approx 1000$. From this last result, we can infer that the increasing force required to form the waves as Bo is augmented is due to the larger viscous dissipation near the interface associated with the presence of the surfactant.[20,21]

The results illustrated in Figure 6b, corresponding to $\Delta\phi_0$, are for $Pe_S = 7.99 \times 10^4$. $\Delta\phi_0$ is indeed a function of Pe_S; nevertheless, in the present situation (in the absence of elastic effects), the velocity field is not affected by the distribution of solute; therefore, the only effect of a decreasing Pe_S is a translation of the curve of $\Delta\phi_0$ vs Bo toward larger values of the phase difference (see eqs 18 and A-15).

The phase difference between the temporal evolution of the interfacial concentration of surfactant and the free surface deflections increases with Bo. One might speculate that, as the surface viscosity is augmented, the second term in eq 18, which represents the convective transport of surfactant, diminishes and, thus, the interfacial distribution of surfactant becomes more and more dependent on surface diffusion. However, we have already mentioned that the shape of the curve of $\Delta\phi_0$ vs Bo is independent of Pe_S; therefore, the phase shift also changes when $Pe_S \ll 1$. Moreover, the solutions of the linear problem (not

presented here) show that γ_n diminishes as Bo is augmented. Therefore, $\Delta\phi_0$ becomes larger because the evolutions of the tangential surface velocity and the free surface deflection becomes out of phase; that is, u_{S_0} approaches zero along the entire interface before the free surface achieves its maximum deformation. At large Bo, the evolutions of free surface height and the maximum absolute value of the tangential component of the free surface velocity are similar to those sketched in Figure 4d, and the concentration of surfactant follows the same trend as $|\tilde{u}_{0,MAX}|$.

From the curves illustrated in Figure 6b, it is easy to notice that the limit achieved by $\Delta\phi_0$ is ∼0.25, i.e., a value significantly smaller than that reported in the previous section, when elastic effects were discussed. This issue has been previously reported when the numerical solution of the full nonlinear problem was discussed.[14]

3.3. Combined Effects of Surface Viscosity and Surface Elasticity. Results discussed in the previous paragraphs show that the force required to form waves on a free surface contaminated with a surfactant conferring elastic or viscous properties to the interface is larger than that on a clean surface. On one hand, the gradient of interfacial concentration of surfactant that accompanies the deformation of the free surface causes a gradient of surface tension that opposes a nonuniform distribution of the surfactant and, consequently, the motion of the liquid. On the other hand, surface viscosity hinders the liquid motion by opposing the nonuniform deformation of the free surface. For sufficiently large values of Ma or Bo, the liquid surface behaves as an incompressible solid surface: as the surface deforms, it bends almost without contracting or expanding.

In this section, we discuss the combined effects of surface viscosity and surface elasticity on the conditions for the onset of the waves. To this end, we built the stability charts on the $F−k$ plane for selected values of Ma, a wide range of Bo, and for $Pe_S = 7.991 \times 10^4$ and 0.7991. From these maps, we determined the values of F_C and k_C for the particular set of parameters chosen. Figure 7a and b shows the evolution of F_C and k_C vs Bo, respectively, when $Pe_S = 7.991 \times 10^4$.

The values of Ma used in the analysis were selected considering the results reported in Figure 2a: the first three values are to the left and the last three to the right of the maximum presented by F_C vs Ma.

The minimum force needed to form the waves as well as the critical wavenumber are not sensitive to variations of surface viscosity at small and large values of Bo. At low Bo, F_C and k_C are dependent on Ma, whereas at large Bo, they attained the limits reported in the previous section; i.e., $F_C \approx 1.40$ and $k_C \approx 0.655$ (see Figures 2 and 5). Moreover, the results illustrated in Figure 3a and in the inset of Figure 7a, show that there exists a range of Ma within which $F_C > 1.4$. The extension of this region is dependent on Bo: it is larger for very small values of this parameter and it is no longer present for $Bo > 100$. Therefore, according to the selected value of Ma, the critical force will either decrease or increase as Bo is augmented. We have noted previously that there is a reverse interfacial flow when surface elasticity rules the behavior of the system; Miles[21] argued that the film back flow, when near in quadrature with the bulk flow, results in an enhanced viscous dissipation, relative to the viscous dissipation produced by an inextensible surface as that formed when the surface viscosity is very large. This larger viscous dissipation leads to a bigger F_C.

The region of Bo within which an increase of this parameter affects the response of the system is dependent on the value of
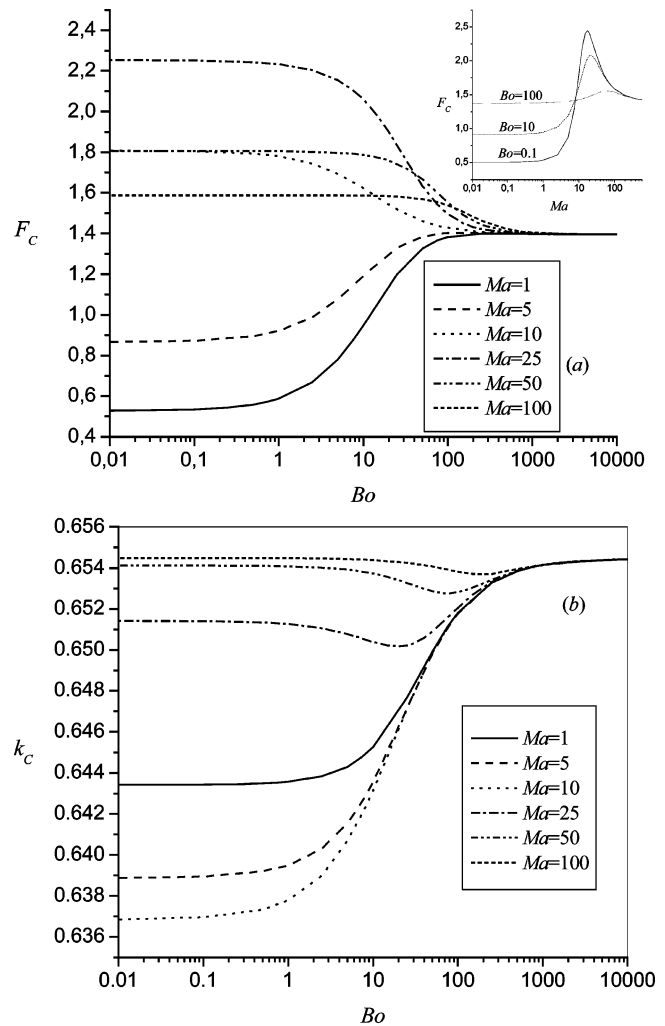

Figure 7. (a) Dimensionless critical force and (b) wavenumber, as a function of Bo for selected values of Ma. Other parameters of the system are $Re = 199.8$, $Ca = 0.0055$, $B = 0.0371$, $z_P = -2.914$, and $Pe_S = 7.991 \times 10^4$.

Ma: the lower limit of this region corresponds to a larger Bo as Ma becomes larger. This fact, together with the nonmonotonic behavior exhibited by F_C, as a function of Ma (see the inset in Figure 7a), leads to the intersection of the curves.

All the curves illustrated in Figure 7b that correspond to the evolution of k_C with Bo merge when this parameter is >400. Another feature of the results reported in this figure is the minimum detected for $Ma = 25$, 50, and 100, which moves toward higher Bo as Ma is augmented.

We also evaluated here the evolution of some interfacial variables, and the results obtained are depicted in Figure 8a−c. As expected, all these variables are dependent exclusively on Ma when the surface viscosity is small; consequently, they present the features described previously for $Bo = 0$; also, they approach a limit that is independent of Ma and Bo when the surface viscosity is large enough. The results illustrated in Figure 8a show that du_{S_0} monotonically decreases as Bo increases, and that the differences due to surface elasticity become less remarkable as Bo becomes larger; therefore, the maximum exhibited by du_{S_0} with Ma for a fixed Bo (see Figure 3b) is noticeable, up to Bo values closer to 20. For $Bo > 400$, the amplitude of the tangential stretching approaches zero for all the systems studied.

The magnitude of the curl of surface velocity versus Bo is illustrated in Figure 8b. For negligible surface viscosity, r_{S_0}, as
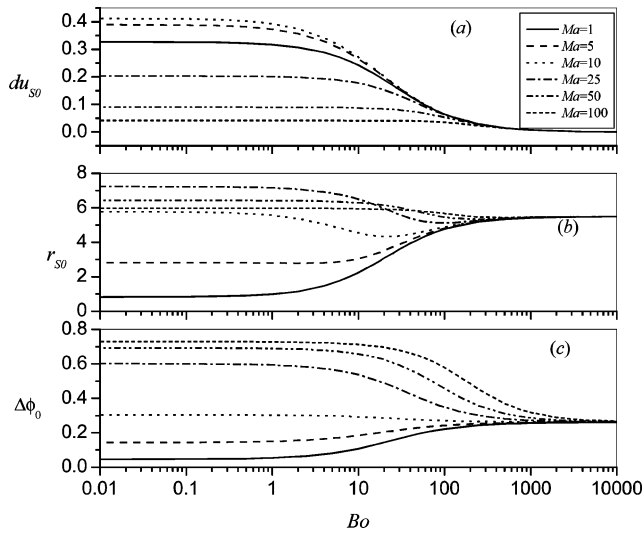
Figure 8. Evolution of (a) du_{S_0}, (b) r_{S_0}, and (c) $\Delta\phi_0$, each as a function of Bo for selected values of Ma. Other parameters of the system are the same as those described in Figure 7.

a function of Ma, follows the nonmonotonic trend reported in Figure 3b, and for large Bo, this property approaches 5.5, which is the value previously reported for the inextensible limit. The most remarkable feature of the curves reported in this figure is the local minimum observed when $Ma > 0.5$; this minimum becomes less important and displaces toward higher values of Bo when Ma is augmented.

The results illustrated in Figure 8c, which correspond to the phase difference between the interfacial concentration of surfactant and the free surface deflections, show that, at low Bo, $\Delta\phi_0$ is dependent only on Ma, but then this variable either decreases ($Ma \leq 5$) or increases ($Ma \geq 10$), until it becomes approximately equal to 0.25 for sufficiently large Bo, independent of Ma. That is, $\Delta\phi_0$ achieves the limit reported already for a system contaminated a surfactant that only confers to the interface viscous effects.

The different behavior of the phase difference results from the competition between elastic and viscous tensions. If $Ma > 20$ and $Bo \ll 1$, the convective transport of solute will reverse before the motion of the liquid in the bulk, and a phase shift even larger than 0.5 (the maximum phase difference attributable exclusively to surface diffusion) can be observed. In this case, an increase of Bo not only diminishes the interfacial velocity but also avoids the asynchronous motion of the interface and the bulk.

If the aforementioned analysis is conducted for $Pe_S = 0.7991$, very similar results are obtained. The more remarkable differences are the disappearance of the minimum in the curves of k_C and the displacement of the minimum values of r_{S_0} toward higher values of both Ma and Bo. These features suggest that elastic effects are less noticeable when the ratio between the magnitudes of diffusion and convection is >1.

4. Conclusion

The linear analysis presented in this work includes the effects of both surface elasticity and surface viscosity on the onset of Faraday waves on a liquid layer of arbitrary depth. Results reported here for typical values of Re, Ca, B, and z_P show that the presence of a surfactant always increases the force required to develop a wavy interface; nevertheless, the nonmonotonic behavior exhibited by F_C vs Ma when the surface viscosity is

negligible and $Pe_S > 1$ is not longer observed when the surface viscosity dominates the dynamics of the system. Also, whenever the critical force passes through a maximum, the critical wavenumber passes through a minimum (though not simultaneously); therefore, in this case, the wavelength of the waves formed in a contaminated surface can be slightly larger than that for a clean interface.

The study that has been performed notes that, in the limit of either very high elasticity or very high viscosity, the free surface deforms in a manner similar to that of a solid plate; that is, it bends almost without contracting or expanding. The only difference observed is the smaller value of the phase difference between the variations of surfactant concentration and the free surface deflections for large Bo and low Ma, compared to that attained at large Ma and small Bo.

We also showed how the evaluation of interfacial properties such as the amplitude of the tangential surface stretching and of the curl of the surface velocity contribute to a better understanding of the behavior of the system.

Appendix. Computation of the Interfacial Variables

The phase shift ($\Delta\phi_n$) between the corresponding time-periodic modes of the interfacial concentration of surfactant ($\hat{\gamma}_n$) and the deflection of the free surface ($\hat{h}_n$) was calculated for the case $n = 0$ (fundamental subharmonic mode), following the methodology presented in Appendix B of ref 9. Besides, to evaluate the influence of the presence of surfactants on the velocity field, the amplitude of the horizontal divergence and the curl of the surface velocity were calculated. With this purpose, and without losing generality, the x-axis was taken along the direction of the wavevector (**k**); then, $\nabla_H \cdot \mathbf{v}^0 = \partial u/\partial x$ and $\nabla \times \mathbf{v}^0 = (\partial u/\partial z - \partial w/\partial x)_{z=0}\mathbf{j}$.

Very briefly, the calculation of $\nabla_H \cdot \mathbf{v}$ is described next. The continuity equation implies

$$\nabla_H \cdot \mathbf{v}_0 + \frac{\partial w}{\partial z} = 0 \Rightarrow \frac{\partial u}{\partial x} = -\frac{\partial w}{\partial z} \qquad \text{(A-1)}$$

where

$$w = e^{ikx}\hat{w}(z, t)$$

$$\hat{w} = \sum_{n=0}^{\infty} [\hat{w}_n(z)e^{i(1/2+n)t} + \hat{w}_n^*(z)e^{-i(1/2+n)t}] \qquad \text{(A-2)}$$

where $\hat{w}_n^*$ is the complex conjugate of $\hat{w}_n$.

From eq A-2, and with a procedure similar to that used in ref 7 to calculate $\Delta\phi_0$, the following expression can be obtained:

$$\frac{\partial w}{\partial z} = 2e^{ikx}\sum_{n=0}^{\infty}\left|\frac{d\hat{w}_n}{dz}\right|\cos\left[\left(\frac{1}{2}+n\right)t + \tilde{\phi}_n\right] \qquad \text{(A-3)}$$

Therefore, the amplitude of $\partial w/\partial z$ in $z = 0$ is dependent on the modulus of $d\hat{w}_n/dz|_{z=0}$, which is evaluated by taking into account that $d\hat{w}_n/dz|_{z=0} = -kb_n + q_nd_n$, where

$$-kb_n + q_n d_n = k\{[\hat{h}_n(-3k^4 + 2k^2qn^2 + q_n{}^4) +$$
$$2\hat{\gamma}_n k^2 MaRe]q_n[-1 + \cosh(kz_P)\cosh(q_n z_P)] +$$
$$k[\hat{h}_n(k^4 + 2k^2qn^2 - 3q_n{}^4) -$$
$$\hat{\gamma}_n(k^2 + q_n{}^2)MaRe]\sinh(kz_P)\sinh(q_n z_P)\} \div \text{DENO} \quad \text{(A-4)}$$

$$\text{DENO} = Re[(q_n{}^2 - k^2)f_n + kBoe_n] \qquad \text{(A-5)}$$

$$f_n = q_n \cosh(q_n z_P)\sinh(kz_P) - k\sinh(q_n z_P)\cosh(kz_P) \quad \text{(A-6)}$$

$$e_n = 2k^2 q_n[1 - \cosh(q_n z_P)\cosh(kz_P)] +$$
$$k(k^2 + q_n{}^2)\sinh(q_n z_P)\sinh(kz_P) \quad \text{(A-7)}$$

In the aforementioned expressions, $\hat{h}_n$ is the $(n+1)th$ component of the eigenvector corresponding to the largest eigenvalue, and $\hat{\gamma}_n$ is evaluated with eq 25. It is important to note that, in the routine used to solve the problem, the eigenvectors are scaled so that the norm of each is equal to one; therefore, values of the interfacial properties are referenced to unity and not to the actual amplitude of the free surface deformation.

The calculations performed indicate that $d\hat{w}_0/dz|_{z=0} \gg d\hat{w}_n/dz|_{z=0}$ for $n > 1$; thus, the amplitude of $\partial w/\partial z|_{z=0}$ can be represented by the first term of the series in all the results shown in this work.

Concerning the magnitude of the curl of surface velocity, it can be easily verified, from eqs A-1 and A-2, that

$$\frac{\partial w}{\partial x} = ike^{ikx}\hat{w}(t,z) \qquad \text{(A-8)}$$

$$u = -\frac{e^{ikx}}{ik}\frac{\partial \hat{w}}{\partial z} + f(z,t) \qquad \text{(A-9)}$$

Because there is no mean flow along the horizontal direction, $f(z,t) = 0$. Consequently, from eqs A-8 and A-9,

$$(\nabla \times \mathbf{v})_y = i\left(\frac{1}{k}\frac{\partial^2 \hat{w}}{\partial z^2} - k\hat{w}\right)_{z=0} e^{ikx} \qquad \text{(A-10)}$$

Finally, replacing eq A-2 in eq A-10, we obtain the following expression for the curl:

$$(\nabla \times \mathbf{v})_y = ie^{ikx}\sum_{n=0}^{\infty} 2|\tilde{C}_n|\cos\left[\left(\frac{1}{2}n + t\right) + \hat{\phi}_n\right] \quad \text{(A-11)}$$

In eq A-11, $\tilde{C}_n = i(Re/k)(\delta + n)c_n$ and $\tan\hat{\phi}_n = (\tilde{C}_{n,i}/\tilde{C}_{n,r})$, where

$$c_n = \frac{h_n\{ik^2 Re(\delta + n)[-2f_n + Bok(q_n - l_n)]\} - MaRek^2\hat{\gamma}_n f_n}{\text{DENO}}$$
$$\text{(A-12)}$$

$$l_n = q_n \cosh(kz_P)\cosh(q_n z_P) -$$
$$k\sinh(kz_P)\sinh(q_n z_P) \quad \text{(A-13)}$$

Also, in this case, the results obtained indicate that the magnitude of the curl of the surface velocity is determined by the value of the first coefficient of the series, $|\tilde{C}_0|$. In the text, $|\tilde{C}_0|$ is referenced as r_{S_0}.

It is also useful to take into account that the standing subharmonic solutions are approximately given by

$$h = \hat{h}_0 \exp(\mathbf{k}\cdot\mathbf{x})\exp\left[\left(\frac{i}{2}\right)t\right]$$

$$\gamma = \hat{\gamma}_0 \exp(\mathbf{k}\cdot\mathbf{x})\exp\left[\left(\frac{i}{2}\right)t\right]$$

$$w = \hat{w}_0(z)\exp(\mathbf{k}\cdot\mathbf{x})\exp\left[\left(\frac{i}{2}\right)t\right]$$

Also, in this context, u_H represents the component of the velocity along the direction of the wavevector:

$$u_H = \hat{u}_{H_0}(z)\exp(\mathbf{k}\cdot\mathbf{x})\exp\left[\left(\frac{i}{2}\right)t\right]$$

If these expressions are introduced in eqs 15 and 18, the following equations are easily obtained:

$$\text{angle}(\hat{w}_0(0)) - \text{angle}(\hat{h}_0) = \frac{\pi}{2} \qquad \text{(A-14)}$$

$$\text{angle}(-i\hat{u}_{H_0}(0)) - \text{angle}(\hat{\gamma}_0) = \text{angle}\left(\frac{i}{2} + \frac{k^2}{Pe_S}\right) \qquad \text{(A-15)}$$

We have evaluated $\text{angle}(-i\hat{u}_{H_0}(0)) - \text{angle}(\hat{\gamma}_0)$ instead of angle-$(\hat{u}_{H_0}(0)) - \text{angle}(\hat{\gamma}_0)$, because $\hat{u}_{H_0}(0)$ is spatially shifted by $\pi/(2k)$, with respect to $\hat{w}_0(0)$, $\hat{h}_0$, or $\hat{\gamma}_0$.

Literature Cited

(1) Faraday, M. On the forms and states assumed by fluids in contact with elastic vibrating surfaces. *Philos. Trans. R. Soc. London* **1831**, *121*, 319.

(2) Miles, J.; Henderson, D. Parametrically forced surface waves. *Ann. Rev. Fluid Mech.* **1990**, *22*, 143.

(3) Miles, J. On Faraday waves. *J. Fluid Mech.* **1993**, *248*, 671.

(4) Perlin, M.; Schultz, W. W. Capillary effects on surface waves. *Ann. Rev. Fluid Mech.* **2000**, *32*, 241.

(5) Goodridge, C. L.; Hentschel, H. G. E.; Lathrop, D. P. Breaking Faraday waves: Critical slowing of droplet ejection rates. *Phys. Rev. Lett.* **1999**, *82*, 3062.

(6) Dobre, M.; Bolle, L. Practical design of ultrasonic spray devices: experimental testing of several atomizer geometries. *Exp. Therm. Fluid Sci.* **2002**, *26*, 205.

(7) Henderson, D. Effects of surfactant on Faraday-wave dynamics. *J. Fluid Mech.* **1998**, *365*, 89.

(8) Decent, P. The nonlinear damping of parametrically excited two-dimensional gravity waves. *Fluid Dynam. Res.* **1997**, *19*, 201.

(9) Kumar, S.; Matar, O. K. On the Faraday instability in a surfactant-covered liquid. *Phys. Fluids* **2004**, *16*, 39.

(10) Kumar, S.; Matar, O. K. Erratum: "On the Faraday instability in a surfactant-covered liquid" [Phys. Fluids 16, 39 (2004)]. *Phys. Fluids* **2004**, *16* (8), 3239.

(11) Matar, O. K.; Kumar, S.; Craster, R. V. Nonlinear parametrically excited surface waves in surfactant-covered thin liquid films. *J. Fluid Mech.* **2004**, *520*, 243.

(12) Kumar, S.; Matar, O. K. Instability of long-wave disturbances on gravity-modulated surfactant-covered thin liquid layers. *J. Fluid Mech.* **2002**, *466*, 249.

(13) Ubal, S.; Giavedoni, M. D.; Saita, F. A. Elastic effects of an insoluble surfactant on the onset of two-dimensional Faraday waves: A numerical experiment. *J. Fluid Mech.* **2005**, *524*, 325.

(14) Ubal, S.; Giavedoni, M. D.; Saita, F. A. The influence of surface viscosity in two dimensional Faraday waves. *Ind. Eng. Chem. Res.* **2005**, *44*, 1090.

(15) Edwards, D. A.; Brenner, H.; Wasan, D. T. *Interfacial Transport Processes and Rheology*; Butterworths—Heinemann: Boston, 1991.

(16) Slattery, J. C. *Interfacial Transport Phenomena*; Springer—Verlag: New York, 1990.

(17) Scriven, L. E. Dynamics of a fluid interface. *Chem. Eng. Sci.* **1960**, *12*, 98.

(18) Stone, H. A. A simple derivation of the time-dependent convective−diffusive transport equation for surfactant transport along a deforming interface. *Phys. Fluids A* **1990**, *2*, 111.

(19) Kumar, K.; Tuckerman, L. Parametric instability of the interface between two fluids. *J. Fluid Mech.* **1994**, *279*, 49.

(20) Levich, V. G. *Physicochemical Hydrodynamics*; Prentice Hall: Englewood Cliffs, NJ, 1962.

(21) Miles, J. W. Surface-wave damping in closed basins. *Proc. R. Soc. London A* **1967**, *297*, 459.

(22) Huber, P.; Soprunyuk, V. P.; Embs, J. P.; Wagner, C.; Deutsch, M.; Kumar, S. Faraday instability in a surface-frozen liquid. *Phys. Rev. Lett.* **2005**, *94*, 184504.